Journal of Achievements in Materials and Manufacturing Engineering
VOLUME 37
ISSUE 2
December
2009

The mechanical characteristics of phosphate glasses under high temperature and friction-induced cross-linking processes

Z. Pawlak [a,b,*], P.K.D.V. Yarlagadda [a], R. Frost [a], D. Hargreaves [a]
[a] Queensland University of Technology, School of Engineering Systems, GPO Box 2434 Brisbane, Q 4001, Australia
[b] Biotribology Laboratory, University of Economics, ul. Garbary 2, 85-229 Bydgoszcz, Poland
* Corresponding author: E-mail address: zpawlak@xmission.com

Received 29.09.2009; published in revised form 01.12.2009

Properties

ABSTRACT

Purpose: In the present study, we consider mechanical properties of phosphate glasses under high temperature-induced and under friction-induced cross-linking, which enhance the modulus of elasticity.
Design/methodology/approach: Two nanomechanical properties are evaluated, the first parameter is the modulus of elasticity (E) (or Young's modulus) and the second parameter is the hardness (H). Zinc meta-, pyro - and orthophosphates were recognized as amorphous-colloidal nanoparticles were synthesized under laboratory conditions and showed antiwear properties in engine oil.
Findings: Young's modulus of the phosphate glasses formed under high temperature was in the 60-89 GPa range. For phosphate tribofilm formed under friction hardness and the Young's modulus were in the range of 2-10 GPa and 40-215 GPa, respectively. The degree of cross-linking during friction is provided by internal pressure of about 600 MPa and temperature close to 1000ºC enhancing mechanical properties by factor of 3 (see Fig. 1).
Research limitations/implications: The addition of iron or aluminum ions to phosphate glasses under high temperature - and friction-induced amorphization of zinc metaphosphate and pyrophosphate tends to provide more cross-linking and mechanically stronger structures. Iron and aluminum (FeO_4 or AlO_4 units), incorporated into phosphate structure as network formers, contribute to the anion network bonding by converting the P=O bonds into bridging oxygen. Future work should consider on development of new of materials prepared by sol-gel processes, eg., zinc (II)-silicic acid.
Originality/value: This paper analyses the friction pressure-induced and temperature–induced the two factors lead phosphate tribofilm glasses to chemically advanced glass structures, which may enhance the wear inhibition. Adding the coordinating ions alters the pressure at which cross-linking occurs and increases the antiwear properties of the surface material significantly.
Keywords: Mechanical phosphate strength; Friction-induced cross-linking; Young's modulus

Reference to this paper should be given in the following way:
Z. Pawlak, P.K.D.V. Yarlagadda, R. Frost, D. Hargreaves, The mechanical characteristics of phosphate glasses under high temperature and friction-induced cross-linking processes, Journal of Achievements in Materials and Manufacturing Engineering 37/2 (2009) 458-465.

1. Introduction

Phosphate glasses are potential candidates for many technological applications, e.g., in optical data transmission, solid-state batteries, sensing and laser technology, nuclear technology, and auto-industry. Their properties such as low melting point, high thermal expansion, mechanical and thermal stress, high chemical durability and aqueous corrosion resistance have been reported. Better understanding of the mechanical properties of phosphate glasses could lead to broader applications by improving composition of glasses [1, 2, 3, 4].

The structure and valence states of the iron ions in these glasses were investigated using Mossbauer spectroscopy, X-ray diffraction, and infrared spectroscopy. X-ray diffraction indicates that the local structure of zinc-iron phosphate is related to the short range structures of crystalline $Zn_2P_2O_7$, $Fe_3(P_2O_7)_2$ and $Fe(PO_3)_3$. The zinc-iron-phosphate glasses can consist of PO_4 tetrahedral joined together by oxygen and contain Fe (II) and Fe (III) and Zn^{2+} ions which act as a modifier in the glass network [1].

The general structure of the zinc-iron-phosphate glasses can be visualized as consisting of PO_4 tetrahedra joined together by oxygen which contain Fe(II) and Fe(III) and Zn(II) ions, these ions act as a modifier in the glass network. Much structural work has been carried out on phosphate glasses in last decade [5-8]. The structure of iron phosphates [9,10] contains di- and tri-valent ions in octahedral coordination, and also contains $(Fe_3O_{12})^{16-}$ clusters. Some phosphate glasses with no monovalent ions, and with the of di- and trivalent oxides (iron pyrophosphate and Zn-Al-metaphosphate) have Young's modulus (70-80 GPa) and tensile strength (S ~ 6 GPa) [5].

It was experimentally confirmed that the addition of metal oxides, e.g., SnO, PbO, ZnO, Fe_2O_3 and Al_2O_3 , results in formation of Sn-O-P, Pb-O-P, Zn-O-P, Fe-O-P and Al-O-P bonds and leads to dramatic improvements in the mechanical properties [1, 5, 11] and in chemical durability of the modified phosphate glasses [12].

Phosphorus compounds under high temperature and friction-induced cross-linking undergo the structural transformation from solid system to amorphous state [13]. The friction-induced activation processes of metallic surface in the presence of Fe(II) form a mixed iron/zinc orthopolyphosphate glass layer, $Fe_2Zn(PO_4)_2$. Young's modulus and hardness are used for mechanical characterization of polyphosphate tribofilm, which in general has a thickness of ~ 100 nm. The tribofilm forms antiwear pads in contacting-rubbing areas of surfaces [18-23].

In the present study, we have considered properties of phosphate glasses and phosphate tribofilm glasses under high temperature- and friction-induced cross-linking conditions. Two nanomechanical properties of phosphate glasses and phosphate tribofilms are evaluated. The first one is the modulus of elasticity (E) (or Young's modulus), which is proportional to the force required to deform a sample elastically. The second parameter is hardness (H), which is a measure of material's resistance to plastic flow.

2. Mechanical properties of phosphate glasses under temperature-induced cross-linking processes

The mechanical strength of phosphate glasses, the tensile strength, and Young's modulus are presented in Table 1 and are compared with phosphate tribofilms generated during friction-induced processes, the comparison is presented in Table 2. The zinc-iron-aluminium-phosphate glasses were prepared by melting homogeneous mixtures of reagent at temperatures between 1000–1200 ^{o}C. Young's modulus of the phosphate glasses is in the 60 - 89 GPa range, the value for the iron phosphate glasses is 69 GPa. The iron free glass Na-Al-P has the lowest modulus of 60 GPa. Young's modulus for the Na-Al-Fe-P and Na-Fe-P fibres increased to 68 and 69 GPa, respectively. Young's modulus of the Zn-Al-Fe-P glass varied little with iron content, but the Zn-Al-P glass had the highest modulus at 89 GPa. Young's modulus of the Zn-Al-Fe-P glasses appears to be higher than that of Na-Al-Fe-P glasses (see Table 1) [1].

The tensile strength of the phosphate glasses falls into two categories. The Zn-Al-Fe-P glass has a tensile strength in the 4.2-7.2 GPa range while the tensile strength of the Na-Al-Fe-P fibres is in the range 2.8-4.2 GPa. A similar increase in tensile strength is observed for a $Zn(PO_3)_2$ (2.4 GPa) compared to that of $NaPO_3$ glass (1.8 GPa). This increase in strength is believed to be due to the replacement of monovalent sodium ions by divalent zinc ion, which increases the cross-link density structure and makes the glass stronger. Zinc aluminophosphate (Zn-Al-P) glasses have a higher tensile strength than the zinc iron phosphate (Zn-Fe-P) glasses. The mechanical strength of phosphates ($NaPO_3$, $Zn(PO_3)_2$ and pyrophosphates glasses (P_2O_7) have been summarized in Table 1.

The small magnitude of all the mechanical properties of $NaPO_3$ can be simply understood when one considers that the structure consists of P-O chains with Na-O-P bonds. Replacing monovalent sodium by divalent zinc results in increase in tensile strain and Young's modulus, presumably because of the cross-linking by divalent cations, while trivalent cations tend to provide either more cross-linking, or perhaps even the formation of stronger structures, e.g., rings or clusters [26].

The iron-phosphorous-oxygen network becomes stronger with increasing Fe_2O_3 content. The improved durability with increased iron content is attributed to the easy hydrated P-O-P bonds being replaced by more chemically resistant Fe-O-P bonds. The O/P ratio is also an important factor to the aqueous chemistry durability as indicated by the 40 Fe_2O_3 – 60P_2O_5 glass which had the best chemical durability. Since this glass had an O/P ratio 3.42, it is expected to contain primarily P_2O_7 groups. The IR and Mossbauer spectra indicate that these glasses are dominated by $(P_2O_7)^{4-}$ dimmer units and contain a large number of Fe (II)-O-P and Fe (III)-O-P bonds, where both Fe (II) and Fe (III) ions have oxygen neighbours in either octahedral or distorted octahedral coordination [12]

Various structure studies of $Zn(PO_3)_2$ glasses indicate that the what Zn coordination is intermediate, between four-coordinated and six-coordinated and has a very large degree of cross-linking [13, 26]. It has been shown that the main factor determining the strength

of glasses is the degree to which their anion network is bonded. Iron and aluminum as FeO_4 or AlO_4 units can be incorporated into phosphate structure as a network formers and contribute to the anion network bonding by converting the P=O bonds into bridging oxygen. Zinc ions are octahedrally coordinated to nearby oxygen ions, they can increase the cross-linking in the glasses structure and thus increase its strength [1, 13, 26].

The small magnitude of all the mechanical properties of $NaPO_3$ can be simply understood when one considers that the structure consists of P-O chains with Na-O-P bonds. Replacing monovalent sodium by divalent zinc results in increase in tensile strain and Young's modulus, presumably because of the cross-linking by divalent cations, while trivalent cations tend to provide either more cross-linking, or perhaps even the formation of stronger structures, e.g., rings or clusters [26].

The iron-phosphorous-oxygen network becomes stronger with increasing Fe_2O_3 content. The improved durability with increased iron content is attributed to the easy hydrated P-O-P bonds being replaced by more chemically resistant Fe-O-P bonds. The O/P ratio is also an important factor to the aqueous chemistry durability as indicated by the 40 Fe_2O_3 – 60P_2O_5 glass which had the best chemical durability. Since this glass had an O/P ratio 3.42, it is expected to contain primarily P_2O_7 groups. The IR and Mossbauer spectra indicate that these glasses are dominated by $(P_2O_7)^{4-}$ dimmer units and contain a large number of Fe (II)-O-P and Fe (III)-O-P bonds, where both Fe (II) and Fe (III) ions have oxygen neighbors in either octahedral or distorted octahedral coordination [12].

Table 1.
Mechanical strength of phosphate glasses prepared by melting processes [1, 5]

Phosphate glass	Tensile strength[a] (S) [GPa]	Young's modulus[b] (E) [GPa]	Young's modulus test method [b]
$Na\ PO_3$	1.8	35.7	3-point bending
$Zn\ (PO_3)_2$	2.4	42.0	3-point bending
$Fe_4(P_2O_7)_3$	5.9	69.5	3-point bending
15 ZnO-17.5 Al_2O_3- 67.5 P_2O_5	5.7	79.0	3-point bending
K-La-P	2.4	47.7	3-point bending
Na-Al-P	2.8	60.0	3-point bending
Na_2O-Fe_2O_3-P_2O_5	2.8	69.0	3-point bending
ZnO-Fe_2O_3- P_2O_5	4.3	68.0	3-point bending
ZnO-Al_2O_3- Fe_2O_3- P_2O_5	5.4	72.0	3-point bending
E-glass	5.8	70.0	3-point bending
S-glass	8.4	87.0	3-point bending

[a] tensile strength test: the 2-point bending (S) = 1.198 E.d/ (D-d), where d is the fibre diameter and D is the separation of the 2-point bending plates at failure [24];
[b] Young's modulus, $E = L^3P/ 48\ S.I$, where P is the load applied, S is the deflection, and I is a moment of inertia about the neutral axis for cylindrical samples ($3.14d^4/4$) [25].

Table 2.
Mechanical properties of phosphate tribofilms obtained under friction-induced cross-linking using 4-ball wear machine

Polyphosphate tribofilm from ZDDP wear tester on steel surfaces	Hardness[a] GPa	Young's modulus (E) [GPa]	Young's modulus[d] methods of determination
ZDDP [33]	nd	81	IFM
ZDDP [34]	nd	209 and 87[c]	IFM
Aryl-ZDD P [34]	nd	50	IFM
ZDDP [39]	10 and 6[b]	215 and150[b]	AFM
MoDTC/ZDDP [39]	10 and 6[b]	215 and150[b]	AFM
ZDDP [46]	2	40	SFA
Sulfide-oxide [46]	4.7	90	SFA
ZDDP [43]	nd	66	AFM
ZDDP, Al-Si [43]	nd	103	AFM
ZDDP [44]	nd	112 and 54[c]	IFM
ZDDP [45]	nd	81	IFM
ZDDP [23]	3.9	96	SFM
ZDDP [30]	nd	140	calculated
ZDDP-Al-Si [30]	nd	70	calculated

[a] (nd) not determined;
[b] when thickness was reduced from 100 nm to 30 nm hardness and modulus decreased;
[c] large plateaus and valleys;
[d] IFM = interfacial - force microscopy; AFM = atomic-force microscopy; SFA = surface force apparatus; SFM = scanning force microscopy.

3. Mechanical properties of phosphate tribofilm under friction-induced cross-linking processes

Two nanomechanical properties of phosphate tribofilms under friction-induced cross-linking are evaluated. The first one is the modulus of elasticity (E) (or Young's modulus). The second parameter is hardness (H). Recently, nanoindentation methods and spectroscopic techniques have been used to determine mechanical properties of the tribofilm. Formation of the chemically durable zinc phosphates tribofilm indicates the presence of heavy metals ions as a modifier of the phosphate network formed during friction processes. The addition of iron or aluminum ions to phosphate tribofilm tends to provide more cross-linking and mechanically stronger phosphate structure [11, 27, 28, 29].

The tribofilm has been identified as being composed of a few distinct regions: large antiwear pads, smaller antiwear pads, and lower lying valley regions between the antiwear pads. The larger antiwear pads correspond to the two contacting (rubbing) surfaces. The thickness and mechanical parameters of tribofilm depend on the load and sliding speed during the wear test.

Differences in determined values of mechanical properties are related to lack of unification of such factors as load, speed, duration time, oils temperature and material during the wear test. Also, tribofilm various thicknesses were measured in the range 150 to 30 nm. Mechanical properties of zinc phosphate tribofilm showed that hardness (2 - 10 GPa) and Young's modulus are thickness-dependent [28]. The Young's modulus values obtained for large and small antiwear pads are in the range of 30 - 215 GPa as shown in Table 2.

The highest degree of cross-linking occurs at the tops of the pads, where the phosphates and metals are exposed to the highest friction-induced pressures. Much smaller pressure and cross-linking occurs in the valleys, which results in much lower indentation modulus. Cross-linking occurs within zinc phosphorus in the presence of Fe ions through formation of Zn-O and Fe-O bonds, which requires sufficient contents of oxygen compounds. The formation of the highly cross-linked network increased the mechanical hardness [30].

It is acceptable, that tribofilms grow from decomposition products rather than from intact ZDDP molecules. In this work we have examined tribofilm which are generated in a standard wear tester. The tribofilm should possess a high hardness to Young's modulus ratio, and value should be far less than that of steel [31]. The literature value of Young's modulus for steel is 220 GPa [32]. The measured Young's modulus value for the ridge region, which corresponds to glassy material, was 81 GPa [33]. The normal load was maintained at 220 N during the wear test, which corresponded to an initial maximum apparent contact pressure of 590 MPa on the basis of Hertz theory for the cylinder-on-flat contact geometry [31].

Mechanical properties testing with an interfacial force microscope (IFM) revealed that the elastic modulus and hardness of the elevated flat regions differed significantly from the surrounding areas. The Young's modulus of tribochemical films derived from zinc dialkyl- and diaryldithiophosphates has been determined as: 87 and 50 GPa for large antiwear pads, respectively, and 209 GPa for the highly loaded the center region of the pad for ZDDP tribofilm [34].

The Young's modulus values for the phosphate tribofilm glasses and phosphate glasses as a function of degree of cross-linking (DCL) are shown in Fig.1. The representation of Young's modulus against values of DCL was plotted on scale from 1 to 10. For phosphate glasses lowest modulus has sodium phosphate value, $NaPO_3$ = 35.7 GPa (for DCL = 1) and serves as a starting point. Highest modulus for phosphate glasses is for S-glass with 87 GP (DCL = 10) (see Table 2).

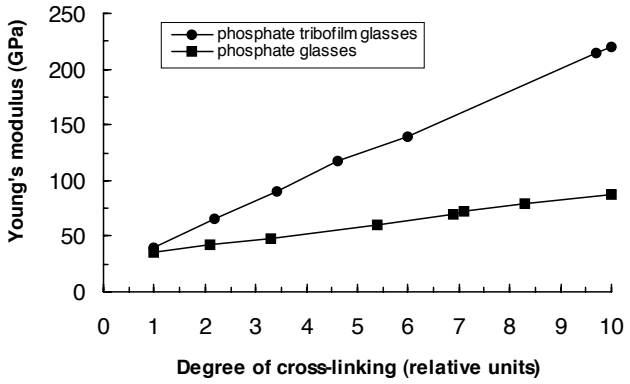

Fig. 1. The Young's modulus of the phosphate tribofilms and phosphate glasses as a function of degree of cross-linking (DCL)

For phosphate tribofilm glasses lowest modulus is 40 GPa (DCL = 1), and highest modulus is for steel with 220 GPa (DCL = 10). From curve slopes comparison we can conclude that phosphate tribochemical glasses have advantage over phosphate glasses of enhancing mechanical properties by factor of 3 (see Fig 1).

The molybdenum dialkyldithiocarbamate (MoDTC) / zinc dialkyldithiophosphate (ZDDP) additive mixture was reported to possess a much lower friction coefficient than a ZDDP tribofilm formed only from the ZDDP additive [35-38]. Both tribofilms the MoDTC/ZDDP and ZDDP possessed the same hardness of 10 GPa and the modulus of 215 GPa when the contact depth was greater than 20 to 30 nm.

The MoDTC/ZDDP and ZDDP tribofilms exhibited different mechanical properties near the surface, the hardness decreased from 10 to 6 GPa and the modulus decreased from level of 215 to 150 GPa. In the elastic deformation range near the surface, the MoDTC/ZDDP tribofilm possessed lower modulus and hardness than ZDDP tribofilm. The SFA and AFM results are not always directly comparable because of the different experimental and samples preparation conditions [39]. Mechanical properties of nanoindentation modulus of phosphate tribofilm glasses are listed in Table 2.

The zinc (II) ion is known to adopt four and six coordination sites with a tetra- and octahedral configuration [13, 26, 30].

Mechanical properties of phosphate glasses formed under high temperature and under friction-induced phosphates on metal

surfaces have many similarities. Nanohardness and nano-indentation modulus measurements carried out on phosphates tribofilm showed that friction and wear behavior was not correlated to their tangenial elastic properties. Instead, they were thought more likely to depend on the different microstructures of the tribofilms [40]. The tribofilms formed on steel shows a bilayer structure with long-chain phosphates at the surface and short-chain polyphosphates ($Zn_2P_2O_7$) found closer to the metal interface. Nascent aluminum was responsible for reacting with ZDDP and forming phosphide AlP and linkage isomer species of ZDDP [40-43].

The measured Young's modulus tribofilms were characterized by large smooth plateaus with value of 112 GPa and surrounding valleys with value of 54 GPa [44]. Indentation performed along a large antiwear pad gave an indentation modulus of 81 GPa [45]. The nanomechanical properties markedly differed, and these differences lie in the extent of involvement of iron ions into polyphosphate glasses [14-17, 29, 46-59].

Tetrahedrally coordinated zinc ions at low pressure but octahedrally coordinated zinc ions at high pressure characterize the structure of zinc phosphate glass. The transformation from tetrahedral to octahedral coordination in zinc phosphate glass occurs at pressures above 17 GPa at room temperature where the ion coordination increases gradually with increasing pressure [30, 42].

4. Transformation of zinc phosphates in hard-core RMs after decomposition of zinc dialkyldithiophosphate (ZDDP)

The mechanism of decomposition zinc of dialkyldithiophosphate (ZDDP) in oil and metal surfaces is thought to be thermal, oxidative and tribochemical [21, 27].

The result of decomposition is a precipitate which contains 86% of zinc phosphate, 11% of zinc pyrophosphate, and 3% of sulfur compound and is in amorphous-colloidal state [47]. When such colloidal precipitates are placed in mineral oil in presence of surfactants, they are transformed into hard-core reverse micelles, RMs [27]. The term "hard- core reverse-micelles, RMs" is used to describe dispersions containing colloidal core, e.g., carbonate, borate, CuO, Ca-phosphate [27]. Hard-core reverse micelles of zinc metaphosphate, pyrophosphate and orthophosphate were prepared and tested on four-ball machine.

The state of colloidal nanoparticles of zinc phosphates and their interaction with surfactant, is believed to be the result of the mechanism shown in Fig. 2. The examination of colloidal precipitates from ZDDP decomposition and powder mixture of zinc metaphosphate and zinc pyrophosphate salts in ratio (9:1) in mineral oil in a 4-ball wear machine, provided comparable antiwear protection [47]. However, the antiwear effectiveness of phosphate powder in mineral oil in engine failed antiwear protection tests. The state of colloidal nanoparticles or amorphous zinc phosphates may be a critical parameter for effectiveness of antiwear performance.

Hard-core reverse micelles of zinc metaphosphate, pyrophosphate and orthophosphate were prepared under conditions such that zinc phosphates were formed by a chemical reaction ($ZnCl_2$ + with sodium meta-, ortho- and pyrophosphates) in presence of oleic acid/or calcium benzenesulfonate as the surfactant (see Fig 3). Then colloidal solution was dispersed in hydrocarbon oil. The concentration of micellar zinc phosphate to oleic acid and mineral oil was 2:2:1,5 [27].

Wear tests run on highly crystalline (powder) zinc meta-, pyro-, and ortho-phosphates on 4-ball machine show good antiwear performance. The physical structure of solid (powder) zinc phosphates and zinc might be a critical property in formation of stable composition in real engine oil. The sizes of powder particles of 40-100 microns are heavy to form hard-core reverse micelles. No antiwear benefit was observed for the phosphates powder addition to engine oil (see Table 3) [27, 47].

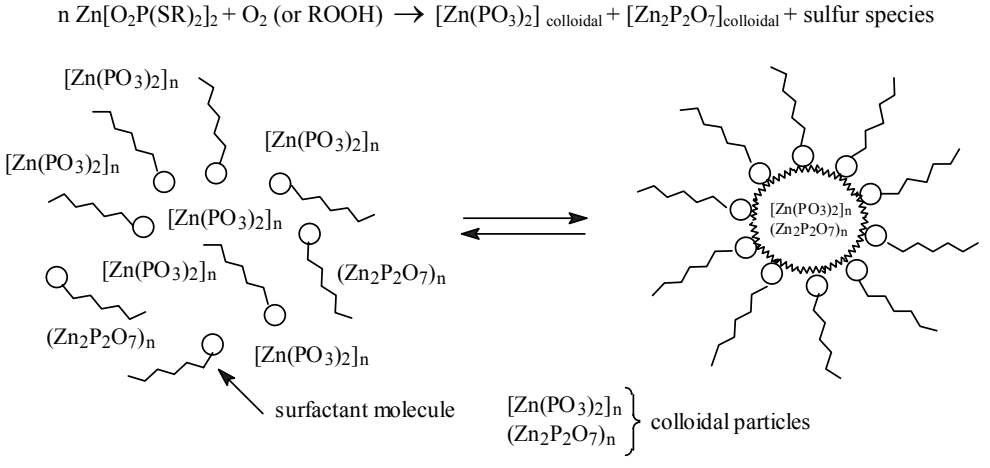

Fig. 2. Formation process of hard-core reverse micelles after decomposition of zinc dialkyldithiophosphate in amorphous/colloidal zinc phosphates $[Zn(PO_3)_2]_n$ and $[Zn_2P_2O_7]_n$

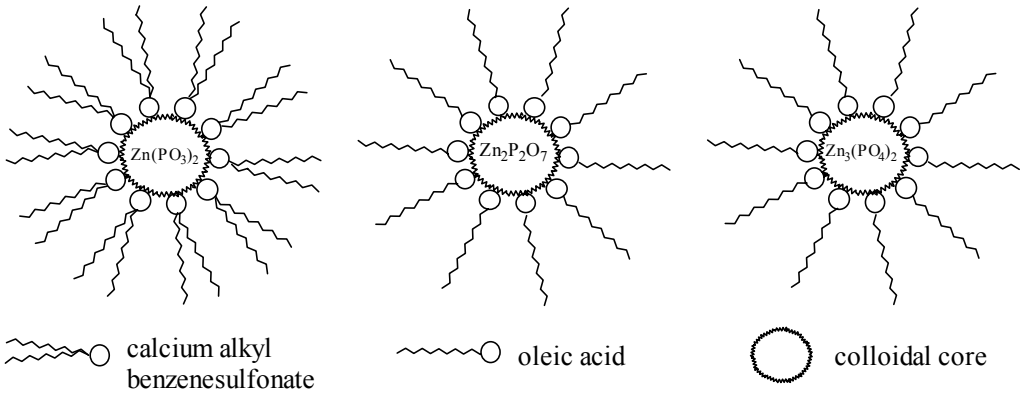

Fig. 3. Schematic representation of phosphate hard-core reverse micelles, RMs, with diameter 10 to 40 nm in hydrocarbon formulation. The mineral core is mainly made up of amorphous phosphate in special procedure of synthesis

Table 3.
Comparison of antiwear performance of zinc dialkyldithiphosphate (ZDDP), zinc metaphosphate ($Zn(PO_3)_2$, pyrophosphate ($Zn_2P_2O_7$) and orthophosphate ($Zn_3(PO_4)_2$) as thermal decomposition products with phosphate solids on 4-ball machine and engine tests

Zinc phosphates	4-Ball machine experiment, Tribofilm formation, (Yes/No)	Engine test, Tribofilm formation (Yes/No)	Tribofilm composition, Zinc-iron polyphosphate (Yes/No)
ZDDP[a]	Yes	Yes	Yes
Zn PO_3/$Zn_2P_2O_7$ [b]	Yes	Yes	Yes
$Zn(PO_3)_2$ [c]	Yes	No[e]	Yes
$Zn_2P_2O_7$ [c]	Yes	No[e]	Yes
$Zn_3(PO_4)_2$ [c]	Yes	No[e]	Yes
$Zn(PO_3)_2$ (micelle)[d]	Yes	Yes	Yes
$Zn_2P_2O_7$ (micelle)[d]	Yes	Yes	Yes
$Zn_3(PO_4)_2$ (micelle)[d]	Yes	Yes	Yes

[a] dissolved in oil;
[b] colloidal phosphate from thermally-decomposed ZDDP;
[c] solid (powder);
[d] hard-core reverse micelles;
[e] sedimentation process.

During thermal decomposition of the ZDDP, amorphous colloidal phosphates nanoparticles are formed and interact with surfactant molecules. The phosphate colloids particles form stable reverse micelles and provide antiwear protection. The existence of colloidal particles, in the presence of surfactants, is also reported in literature as hard-core reverse micelles [27].

5. Conclusions

We have evaluated mechanical properties of the phosphate glasses, which formation is based on temperature-induced cross-linking changes, and have compared them with properties of phosphate tribofilm glasses. The phosphate tribofilm glasses formation is based on friction-induced changes in the coordination of the zinc atoms in the phosphates system, which results in cross-linking through the formation Zn-O bonds. We note, that the most important components in formation of chemically connected network of phosphate glasses and tribofilm glasses are cross-linking agents such as heavy metal. Adding the coordinating ions alters the pressure at which cross-linking occurs and increases the antiwear properties of the surface material significantly. Tribochemical phosphate glasses have advantage over phosphate glasses of enhancing mechanical properties by factor of 3 (see Fig. 1). The degree of cross-linking during friction is provided by internal pressure of about 600 MPa and temperature close to 1000 ^{O}C. These two factors lead phosphate tribofilm glasses to chemically advanced glass structures, which may enhance the wear inhibition

References

[1] M. Karabulut, E. Melnik, R. Stefan, G.K. Marasinghe, C.S. Ray, C.R. Kurkjian, D.E. Day, Mechanism and structural properties of phosphate glasses, Journal of Non-Crystalline Solids 288 (2001) 8-17.
[2] R.K. Brow, Review: the structure of simple phosphate glasses, Journal of Non-Crystalline Solids 263-264 (2000) 1-28.
[3] B.C. Sales, L.A. Boatner, Lead-iron phosphate glass: a stable storage medium for high-level nuclear waste, Science 226 (1984) 45-48.

[4] D.E. Day, Z. Wu, C.S.M. Ray, P. Hrma, Chemically durable iron phosphate glass waste forms, Journal of Non-Crystalline Solids 241 (1998) 1-12.
[5] C.R. Kurkjian, Mechanical properties of phosphate glasses, Journal of Non-Crystalline Solids 263-264 (2000) 207-212.
[6] S.W. Martin, Review of the structures of phosphate glasses, European Journal of Solid State and Inorganic Chemistry, 28 (1991) 164-205.
[7] U. Hoppe, A structural model for phosphate glasses**,** Journal of Non-Crystalline Solids 195 (1966) 138-147.
[8] U. Hoppe, R. Kranold, D. Stachel, A. Barz, A.C. Hannon, A neutron and X-ray diffraction study of the structure of the $La_3P_3O_9$, Journal of Non-Crystalline Solids 232-234 (1998) 44-51.
[9] G.K. Marasinghe, M. Karabulut, C.S. Ray, D.E. Day, M.G .Shumsky, W.B. Yelon, C.H. Booth, P.G. Allen, D.K. Shuh, Structural features of iron phosphate glasses, Journal of Non-Crystalline Solids 222 (1997) 144-152.
[10] M. Ijjaali, G. Venturini, R. Gerardin, B. Malaman, C. Gleitzer, Synthesis, structure and physical properties of a mixed-valence iron diphosphate $Fe_3(P_2O_7)_2$: first example of trigonal prismatic $iron^{(2+)}$ with oxo ligands, European Journal of Solid State and Inorganic Chemistry 28 (1991) 983-998.
[11] T. Jermoumi, S. Hassan, M. Hafied, Ultrafast third-order nonlinear optical spectroscopy of chlorinated hydrocarbons, Vibrational Spectroscopy 32 (2003) 207-213.
[12] S.T. Reis, M. Karabulut, D.E. Day, Chemical durability and structure of zinc–iron phosphate glasses, Journal of Non-Crystalline Solids 292 (2001) 150-157.
[13] R.K. Brow, D.R. Tallant, S.T. Myers, C.C. Phifer, The short-range structure of zinc polyphosphate glass, Journal of Non-Crystalline Solids 191 (1995) 45-55.
[14] G.E. Brown, K.D. Keefer, P.M. Fenn, Extended x-ray absorption fine structure (EXAFS) study of iron-bearing silicate glasses: iron coordination environment and oxidation state, Abstracts of the Geological Society of America 10 (1978) 373.
[15] A. Behrens, H. Schafstall, 2D and 3D simulation of complex multistage forging processes by use of adaptive friction coefficient, Journal of Materials Processing Technology 80-81 (1998) 298-303.
[16] Y.C. Lin, S.W. Wang, T.M. Chen, A study on the wear behavior of hardened medium carbon steel, Journal of Materials Processing Technology 120 (2002) 126-132.
[17] A. Olefinjana, T. Tesfamichael, J.M. Bell, Chemical modification and the attending surface hardness of low alloy steel through medium energy nitrogen ion implantation, Journal of Materials Processing Technology 164-165 (2005) 905-910.
[18] P.A. Willermet, DP. Dailey, R.O. Carter III, P.J. Schmitz, W. Zhu, Mechanism of formation of antiwear films from zinc dialkyldithiophosphates, Tribology International 28/3 (1995) 177-187.
[19] P.A. Willermet, R.O. Carter III, P.J. Schmitz, M. Everson, D.J. Scholl, W.H. Weber, Formation, structure, and properties of lubricants-derived antiwear films, Lubrication Science 9 (1997) 325-348.
[20] J.M. Martin, C. Grossiord, T. Le Mogne, J. Igarashi, Role of nitrogen in tribochemical interaction between Zndtp and succinimide in boundary lubrication, Tribology International 33 (2000) 453-459.
[21] J.M. Martin, Antiwear mechanism of zinc dithiophosphate: a chemical hardness approach, Tribology Letters 6 (1999) 1-8.
[22] S. Corezzi, D, Fioretto, R. Casalini, P.A. Rolla, Glass transition of an epoxy resin induced by temperature, pressure and chemical conversion: a rationale based on configurational entropy, Journal of Non-Crystalline Solids 307-310 (2002) 281-287.
[23] M. Aktary, M.T. DcDermott, G.A. McAlpine, Morphology and nano-mechanical properties of ZDDP antiwear films as a function of tribological contact time, Tribology Letters 12 (2002) 155-161.
[24] M.J. Matthewson, C.R. Kurkjian and S.T. Gulati, Strength measurements of optical fibers by bending, Journal of the American Ceramic Society 69 (1986) 815-821.
[25] T. Klug, R. Bruckner, Preparation of C-fibre borosilicate composities: influence of the fibre on mechanical properties, Journal of Matierals Science 29 (1994) 4013-4021.
[26] E.C. Onyiriuka, Zinc phosphate glass surfaces studied by XPS**,** Journal of Non-Crystalline Solids 163 (1993) 268-273.
[27] Z. Pawlak, Tribochemistry of Lubricating Oils, Elsevier, Amsterdam, 2003.
[28] M.A. Nicholls, T. Do, P.R. Norton, M. Kasrai, G.M. Bancroft, Review of the lubrication of metallic surfaces by zinc dialkyl-dithiophosphates, Tribology International 38 (2005) 15-39.
[29] M. Belin, J.M. Martin, J.L. Mansot, Friction–induced amorphization with ZDDP, Tribology Transactions 32 (1989) 410-413.
[30] N.J. Mosey, M.H. Muser, T.K. Wo, Molecular mechanism for the functionality of lubricant additives, Science 307 (2005) 1612-1615.
[31] K.L. Johnson, Contact Mechanics, Cambridge University, New York, 1985.
[32] J. Tuma, Handbook of Physical Calculations, McGraw-Hill, New York, 1983.
[33] O.L. Warren, J.F. Graham, P.R. Norton, J.E. Houston, T.A. Michalske, Nanomechanical properties of films derived from zinc dialkyldithiophosphate, Tribology Letters 4 (1998) 189-198.
[34] J.F. Graham, C, McCaugue, P.R. Norton, Evaluation of local mechanical properties in depth in MoDTC/ZDDP and ZDDP tribochemical reacted films by using nanoindentation, Tribology Letters 4 (1999) 149-157.
[35] K. Kubo, M. Kibukawa, Y. Skimakawa, The effect on friction of lubricants containing zinc dithiophosphate and organomolybdenum compoud, Proceedings of the IMechE: Part C - Journal of Mechanical Engineering Science C68/85 (1985) 121-131.
[36] Z. Pawlak, P.K.D.V. Yarlagadda, D. Hargreaves, V. Kosse, R. Frost, T. Rauckyte, S. Zak, Mechanism of hardening for the surface phosphates under external high pressure, Proceedings of the 11th International Scientific Conference "Contemporary Achievements in Mechanics, Manufacturing and Materials Science" CAM3S, Gliwice − Zakopane, 2005, 788-792.

[37] M. Kasrai, J.N. Cutler, K. Gore, G.M. Bancroft, K.H. Tan, The chemistry of antiwear films generated by the combination of ZDDP and MoDTC examined by X-ray absorption spectroscopy, Tribology Transactions 41 (1998) 69-77.
[38] J.M. Martin, C. Grossiord, Th. Le Mongne, J. Igarashi, Transfer films and friction under boundary lubrication, Wear 245 (2000) 107-115.
[39] J. Ye, M. Kano, Y. Yasuda, Evaluation of local mechanical properties in depth in MoDTC/ZDDP and ZDDP tribochemical reacted films using nanoindentation, Tribology Letters 13 (2002) 41-47.
[40] J.M. Martin, C. Grossiord, T.L. Mogne, S. Bec, A. Toneck, The two-layer structure of Zndtp tribofilms Part I: AES, XPS and XANES analyses, Tribology International 34 (2001) 523-530.
[41] M.A. Nicholls, P.R. Norton, G.M. Bancroft, K. Fyfe, M. Kasrai, X-ray absorption spectroscopy of tribofilms produced from zinc dialkyl dithiophosphates on Al–Si alloys, Wear 257 (2004) 311-328.
[42] M.M. Robersts, J.R. Wienhoff, K. Grant, D.J. Lacks, Structural transformations in silica glass under high pressure, Journal of Non-Crystalline Solids 281 (2001) 205-212.
[43] M.A. Nicholls, P.R. Norton, G.M. Bancroft, M. Kasrai, G. De Stasio, L.M. Wiese, Spatially resolved nanoscale chemical and mechanical characterization of ZDDP antiwear films on aluminum–silicon alloys under cylinder/bore wear conditions, Tribology Letters 18 (2005) 261-278.
[44] M.A. Nicholls, T. Do, P.R. Norton, G.M. Bancroft, M. Kasrai, T.W. Capehart, T.T. Cheng, T. Perry, Chemical and mechanical properties of ZDDP antiwear films on steel and thermal spray coatings studied by XANES spectroscopy and nanoindentation techniques, Tribology Letters 15 (2003) 241-248.
[45] M.A. Nicholls, P.R. Norton, G.M. Bancroft, M. Kasrai, T. Do, B.H. Frazer, G. DeStasio, Nanometer scale chemomechanical characterization of antiwear films, Tribology Letters 15 (2003) 205-216.
[46] S. Bec, A. Tonck, J.M. Georges, R.C. Coy, J.C. Bell, G.W. Roper, Relationship between mechanical properties and structures of zinc dithiophosphate anti-wear films, Proceedings of the Royal Society of London A 455 (1999) 4181-4203.
[47] A. Molina, Isolation and chemical characterization of a zinc dialkyldithiophosphate-derived antiwear agent, Tribology Transactions 30/4 (1987) 479-485.
[48] J.P. Bricout, P. Hivart, J. Oudin, Y. Ravalard, New testing procedure of zinc phosphate coatings involved in cold forging of cylindrical steel billets, J. Mater. Process. Technol., 24 (1990) 3-12.
[49] C. Wierre, J. D. Guerin, J. Oudin and J. P. Bricout, Finite-element analysis of the initial stage of the indentation-rotation test for phosphate and stearate coatings, Journal of Materials Processing Technology 41 (1994) 171-185.
[50] H.H. Tsai, H. Hocheng, Prediction of a thermally induced concave ground surface of the workpiece in surface grinding, Journal of Materials Processing Technology 122 (2002) 148-159.
[51] W.M. Lima, F.J. Velasco, J. Abenojar, J.M. Torralba, Numerical approach for estimating the elastic modulus in MMCs asa function of sintering temperature, Journal of Materials Processing Technology 143-144 (2003) 698-702.
[52] J.G. Lenard, The effect of lubricant additives on the coefficient of friction in cold rolling, Journal of Materials Processing Technology 80-81 (1998) 232-238.
[53] B. Hum, H.W. Colquhoun, J.G. Lenard, Measurements of friction during hot rolling of aluminum stripes, Journal of Materials Processing Technology 60 (1996) 331-338.
[54] L. Lazzaroto, L. Dubar, A. Dubois, P. Revassard, J. Oudin, Three selection criteria for the cold metal forming lubricating oils containing extreme pressure agents, Journal of Materials Processing Technology 80-81 (1998) 245-250.
[55] J. Monaghan, M. O'Reilly, The influence of lubrication on the surface finish of cold forged components, Journal of Materials Processing Technology 56 (1996) 678-690.
[56] D.-H. Jang, T.-K. Ryou, D.-Y. Yoon, B.-B. Hwang, The process sequence design of a power-assisted steering part, Journal of Materials Processing Technology 113 (2001) 87-92.
[57] H.M. Jiang, X.P. Chen, H. Wu, C.H. Li, Forming characteristics and mechanical parameter sensitivity study on pre-phosphated electro-galvanized sheet steel, Journal of Materials Processing Technology 151 (2004) 248-254.
[58] C. Caminaga, R.L. da Silva Issii, S.T. Button, Alternative lubrication and lubricants for the cold extrusion of steel parts, Journal of Materials Processing Technology 179/1-3 (2006) 87-91.
[59] Z. Pawlak, P.K.D.V. Yarlagadda, R. Frost, D. Hargreaves, The mechanical strength of phosphates under friction-induced cross-linking, Journal of Achievements in Materials and Manufacturing Engineering 17 (2006) 201-204.